BSD-TDR-63-102

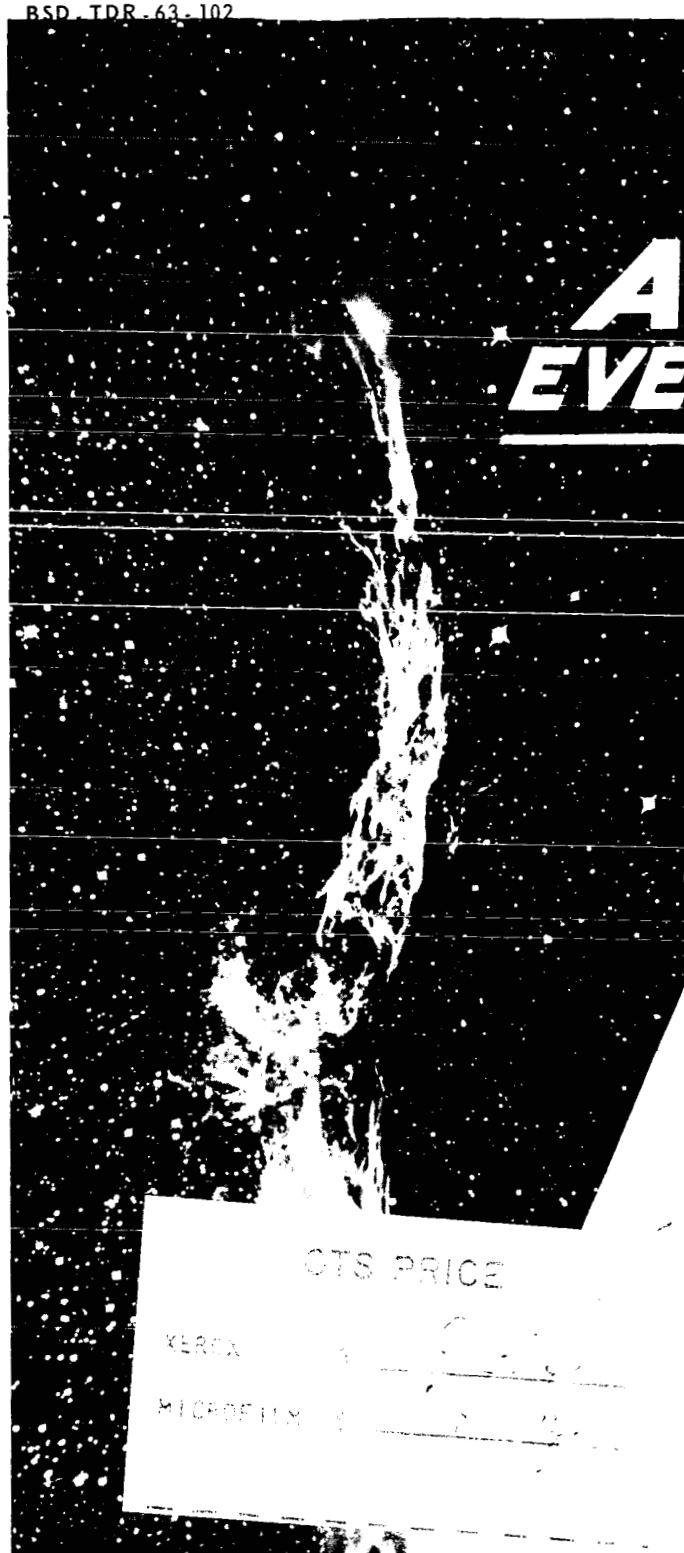

N63 23008
CODE-1
(NASA CR-51805)

AVCO EVERETT RESEARCH LABORATORY

a division of
AVCO CORPORATION

KRAMERS' AND LINE RADIATION FROM NITROGEN AND AIR SHOCKS

R. A. Allen, R. L. Taylor and A. Textoris

AMP 113
May 1963

supported by
HEADQUARTERS
BALLISTIC SYSTEMS DIVISION
AIR FORCE SYSTEMS COMMAND
UNITED STATES AIR FORCE
under Contract No. AF 04(694)-33

ADVANCED RESEARCH PROJECTS AGENCY
monitored by the
ARMY MISSILE COMMAND
UNITED STATES ARMY
under Contract No. DA-19-020-ORD-5476
(part of Project Defender)

NATIONAL AERONAUTICS AND SPACE ADMINISTRATION
MANNED SPACECRAFT CENTER
GENERAL RESEARCH PROCUREMENT OFFICE
under Contract No. NAS 9-858

CTS PRICE
XEROX
MICROFILM

; BSD-TDR-63-102) OTS: ; AMP 113;

KRAMERS' AND LINE RADIATION FROM NITROGEN AND AIR SHOCKS

by

R. A. Allen, R. L. Taylor and A. Textoris

AVCO-EVERETT RESEARCH LABORATORY
a division of
AVCO CORPORATION
Everett, Massachusetts

May 1963 23p 16 refs [12]

supported by

HEADQUARTERS
BALLISTIC SYSTEMS DIVISION
AIR FORCE SYSTEMS COMMAND
UNITED STATES AIR FORCE
Air Force Unit Post Office
Los Angeles 45, California
under Contract No. AF 04(694)-33 and

ADVANCED RESEARCH PROJECTS AGENCY
monitored by the
ARMY MISSILE COMMAND
UNITED STATES ARMY
Huntsville, Alabama
under Contract No. DA-19-020-ORD-5476 (Proj. Defender)
(part of Project Defender)

NATIONAL AERONAUTICS AND SPACE ADMINISTRATION
MANNED SPACECRAFT CENTER
GENERAL RESEARCH PROCUREMENT OFFICE
Houston 1, Texas
(NASA
under Contract No. NAS 9-858;

ABSTRACT

23008

Radiation data are presented which have been obtained from both the nonequilibrium and equilibrium regions behind normal shocks in the velocity range from 7 to 12 mm/μ sec using the recently developed electric arc-driven shock tube. Atomic line radiation is found to be a prominent feature of both the nonequilibrium and equilibrium regions of strong air and nitrogen shocks at wavelengths longer than 0.6μ. For the higher end of this velocity range, molecular band radiation from air is negligible compared to the continuum radiation produced by the capture and the deceleration of electrons (Kramers' radiation). Measurements of this continuum have been made and are found to be in good agreement with theoretical predictions based on calculations performed by Biberman and Norman for the free-bound radiation from nitrogen.

Farther in the infrared from 2 - 8μ, radiation measurements have been made behind reflected shocks in air and nitrogen at equilibrium temperatures of 6 - 9000°K. This continuum radiation is interpreted as due to free-free scattering of electrons from neutral atoms and molecules. An analysis of the data using the classical Kramers' radiation formula has resulted in establishing the "effective coulombic charge," Z, for N_2, N and O, and indicates that in air the bulk of the free-free radiation is due to nitrogen atoms and molecules, with oxygen giving a negligible contribution.

Author

1. Introduction

Previous incident shock radiation measurements below 8 mm/μsec in air and nitrogen had indicated that the bulk of the radiation came from molecular systems with an overshoot region produced at the shock front.[1,16] The present investigation was undertaken to extend the previous incident shock measurements to higher velocities, and to determine the contributions from various classes of radiation. A second part of the investigation was undertaken to extend measurements on reflected shocks farther into the infrared, where the bulk of the radiation is due to free-free scattering of electrons by neutral atoms and molecules and to determine the scattering efficiency of the various atomic and molecular species.

2. Electric Arc-Driven Shock Tube Measurements

Experimental

The electric arc-driven shock tube employed in this study is thoroughly described by Camm and Rose.[3] It is basically the same as a combustion-driven shock tube except for the fact that helium is used for the driver gas and energy is supplied by a condenser bank which discharges through an arc struck coaxially between the diaphragm and the back end of the driver. Photometric measurements on the shock-heated gas were made between .24 and .90μ wavelength using a dual channel monochromator with quartz optics.

Typical photomultiplier records of air shocks are shown in Fig. 1 for initial pressures of 0.1 mm Hg and at three different shock velocities. The measurements shown were made in the .55 to 1.0μ and .40

to .42μ wavelength regions. The time resolution of the optical system was approximately 0.1μ sec. The radiation profiles exhibit a pronounced overshoot and then relax to a relatively steady-state condition interpreted as an equilibrium radiation level. The slight rise in equilibrium radiation as one moves away from the shock front has been attributed to effects of attenuation of the shock velocity.[4] These measurements were made looking through quartz ports mounted in copper knife edges which protruded into the center of the shock tube to eliminate boundary layer effects along the shock tube walls, and to reduce shock curvature, as described by Lin.[5]

A single channel monochromator was used to make measurements in the infrared employing a M-7500 germanium photodiode. A gold-doped germanium detector with a filter was used for measurements at 2.75μ.

Equilibrium Radiation Measurements

Data on the equilibrium intensity of radiation from normal air shocks at 10 mm/μsec at an initial pressure of 0.1 mm Hg are shown in Fig. 2. All the experimental data were obtained at the same shock speed, within 3%, producing an equilibrium temperature of 9650°K and about 10% ionization. In the experiment with the dual channel monochromator, the two intensities obtained in adjacent channels on each run are represented by a solid triangle and open circle connected by a short line. The measurements between 1.0 and 2.0μ were made with the single channel monochromator; the wavelength resolution of which is indicated in the figure.

The prominent features of these equilibrium measurements are the N and O line contributions between 0.6 and 1.5μ and the N_2^+ (1-) molecular band system between 0.3 and 0.5μ. These atomic lines have been

identified spectroscopically in reflected shocks.[6]

Nonequilibrium Radiation

Measurements of the nonequilibrium radiation were made by detailed examinations of radiation profiles, such as those shown in Fig. 1. Parameters, such as time to peak radiation, time for the radiation to fall to a value 10% above the equilibrium level, intensity at peak radiation, peak to equilibrium ratio, and integrated luminous front radiation were all obtained as a function of wavelength. Generally, the nonequilibrium radiation was found to binary scale,[1] as long as the peak to equilibrium intensity ratios were greater than 2. The absolute peak intensities of the radiation at various wavelengths are shown in Fig. 3. Since the units of intensity in this figure are the same as those of the equilibrium measurements in Fig. 2, the peak to equilibrium ratio as a function of wavelength can be obtained by comparing the two figures. For the conditions of these measurements, namely, 10 mm/μsec and initial pressures of 0.1 mm Hg, this ratio was approximately 4 in the visible and essentially unity around 2.0μ. The conclusion that can be immediately drawn from Figs. 2 and 3 is that the atomic line radiation is prominent in both the nonequilibrium and equilibrium regions of strong incident air shocks. The fact that the infrared measurements beyond 1.5μ did not strongly overshoot indicates that Kramers' radiation does not strongly contribute in the nonequilibrium region. This is consistent with the fact that the electron concentration does not strongly overshoot in the nonequilibrium region.[7]

Discussion of Incident Shock Results

The equilibrium conditions produced behind normal shocks can be

calculated from the initial pressure, shock velocity and equilibrium constants for the gas in question. For the present case of air at 10 mm/μsec and initial pressure of 0.1 mm Hg, the equilibrium degree of ionization is about 10% with the molecules being almost completely dissociated. It is evident that for incident shock velocities in excess of 9 mm/μsec, Kramers' and line radiation become increasingly more important as one goes to higher velocities.

Biberman and Norman[8] at the Moscow Power Institute have obtained corrections to the Unsöld-Kramers' formula for radiative recombination using the quantum defect method of Burgess and Seaton.[9] They calculate a quantity $\xi_{(\nu, T)}$ which is a correction factor to the Unsöld equation with $Z_{fb} = 1$. The total continuum radiation becomes

$$\mathcal{E}_{\nu} = 1.63 \times 10^{-35} \frac{N_e N_i}{T^{1/2}} \left[\xi_{(\nu,T)} + (Z^2_{ff} - \xi_{(\nu,T)}) e^{-hc\nu/kT} \right] \frac{\text{watts}}{\text{cm}^2 \text{ ster}} \qquad (1)$$

The quantity $\xi_{(\nu, T)}$ takes into account the capture of the electron to various levels of the nitrogen atom, and it averages over the various electron levels so that the free-bound emission edge structure is lost. Figure 4 presents calculations for the various equilibrium contributors which should be important for the 10 mm/μsec air shock at initial pressure 0.1 mm Hg. The Biberman "total" line is the sum of the Biberman free-bound calculation, plus an Unsöld free-free calculation based on a $Z^2_{ff} = 1$. The calculation for the O_{fb} is based on the photoabsorption measurements of Branscomb, et al.[10] An effective Z^2 of 0.1 is used for the Kramers' radiation due to the scattering of electrons by neutral nitrogen atoms which is discussed in a later section. The

N_2^+ (1-) calculation for these shock conditions is based on the f number of .035 as re-evaluated by Keck, et al.[11] The N_2(2+) calculation is based on an f number of .09.[6] The calculation for the intensity of the nitrogen atom lines at 0.87 and 1.0 with 0.02μ resolution were based on the Einstein coefficients published by J. Richter[12] and do not include the effect of collision limiting. At these wavelengths, the lines are essentially optically thin, since the brightest peak intensity of any of the lines does not exceed 10% of the black body based on their doppler widths. The optical thinness of the gas was also experimentally verified by varying the thickness of the gas sample.

The comparison between the calculations and the data is made in Fig. 2 which shows the Biberman and Norman calculated total radiation excluding atomic line radiation. Comparing the calculations with the data, one concludes that the Biberman and Norman method is essentially correct for obtaining the level of the intensity of radiation in the valleys between the line radiation.

The radiation between .8 and 1.5μ is attributed mainly to atomic N and O line radiation. Calculations of N line radiation contributors at .87μ and 1.0μ in Fig. 4 agree well with measurements. At wavelengths longer than 1.1μ, the oscillator strength for bound-bound transitions of nitrogen and oxygen atoms were not available, and, hence, no calculations for the line radiation have been made in this region.

In conclusion, the important features of strong, incident air shocks in excess of 9 mm/μsec and in the wavelength interval from .25 to 2.0μ are: (1) molecular band radiation contributes increasingly less to

the radiation as one goes to higher velocities, (2) as one goes to higher velocities the atomic line and Kramers' radiation become the important radiators, with the atomic line radiation being the important feature from 0.6μ to 1.1μ and possibly extending farther into the infrared, (3) atomic line radiation "overshoots" in the relaxation region at the shock front.

3. Reflected Shock Measurements

Experimental

The experimental technique is similar to that of Wentink, et al.[2] A combustion-driven, metal shock tube of 1-1/2 inches diameter and 14 ft length was used. To obtain the high temperature and densities of interest, the measurements were made behind the reflected shock. The gas conditions were determined by measuring the incident shock velocity and using the normal shock relation assuming equilibrium conditions behind the reflected shock.[13] To minimize spurious radiation from the boundary layer, the radiation was observed through the end plate along the tube axis with a solid angle such that the near wall was not in the optical path. The radiation was dispersed in a monochromator and was detected with a gold-doped germanium infrared detector. In order to determine the absolute intensity of the emitting gas from the experimental measurements, it was necessary to calibrate the infrared detector against a black body source.

Results

Typical oscillograms of the signals from the IR detector show a linearly increasing signal, as the shock reflects, for the test time of

30-40μsec. If it is assumed that the gas is at a steady, equilibrium temperature and is optically thin, then the linear rise in signal is due to the increase in path length of emitting gas as the reflected shock wave recedes from the end of the tube. At the final densities and temperatures used in this study, the chemical and ionization processes in the gas will be over in well under a microsecond and no relaxation region is detected behind the reflected shock.[13]

The intensity of the equilibrium infrared radiation from shock-heated air, I_λ, as a function of wavelength, λ, is shown in Fig. 5. Each data point is the result of a run at the nominal temperature of 8000°K and 0.90 atmospheric density (initial pressure = 1.0 cm Hg). Runs at temperatures other than 8000°K have been normalized to that temperature using the experimentally measured temperature dependence of the radiation. In the majority of cases this is an adjustment of only a few percent. Most of the data were obtained with a band pass of 0.4μ at 2.0μ and 0.08μ at 6.5μ. Figure 6 shows the wavelength dependence of the infrared radiation from pure nitrogen again normalized to 8000°K and is to be compared with Fig. 5 for air.

The temperature dependence of the infrared radiation from air and nitrogen is shown in Fig. 7 from 6000 - 9000°K at several wavelengths, 2.35μ and 3.88μ for air and 3.07μ for nitrogen. All these runs were carried out at initial pressures of air of 1.0 cm Hg. The range of temperature covered was controlled by the capability of the shock tube at the high temperatures and by the small signal level which was becoming difficult to detect at the low temperatures.

Discussion of Results

The present results for air, Fig. 5, are to be compared with the previous study by Wentink, et al.[2] These authors studied the wavelength region 1 - 4.8μ. The present results are lower than Wentink's by almost a factor of 2 from 2 - 4μ. Beyond 4μ Wentink's data show a large increase in intensity which is not found in the present investigation.

The continuum radiation in the infrared from shock-heated air and nitrogen is attributed to free-free scattering of electrons by neutral atoms and molecules — Kramers' radiation. Unfortunately, the quantum mechanical calculation of this radiation is not well established due to the difficulty of specifying the scattering potential of the neutral species. However, phenomenologically, the results may be compared with the classical Unsold[14,15] expression for Kramers' radiation:

$$I_{\lambda,T} = \frac{16\pi e^6}{3\sqrt{3}\,mc^2}\,(2\pi mkT)^{-1/2}\,\lambda^{-2}\,e^{-hc/kT\lambda}\,[n_e]\sum_i Z_i^2\,[n_i] \qquad (2)$$

where e and m are the charge and mass, respectively, of the electron, $[n_e]$ is the concentration of electrons, Z_i^2 is the "effective coulombic charge" of the neutral species, $[n_i]$, doing the scattering, and the summation is overall species. Z_i is associated with the "strength" of the scattering and should be related to the cross section for elastic scattering of the neutral species. For ions, $Z_i^2 = 1$, $\sum_i [n_i] = [n_e]$, and Eq. (1) goes over into the usual Kramers' expression for highly ionized gases. Calculations indicate that over the temperature range of the present experiment the Kramers' radiation from ionic scattering is

negligible. However, due to the steeper temperature dependence of the ionic scattering over neutral scattering, the former process will dominate at somewhat higher temperatures than considered here, i.e., $> 10,000^{\circ}K$.

If the present measurements are assumed to be due to free-free scattering from neutrals, then the data of Fig. 7 can be analyzed to provide estimates of the effective Z's. Equation (2) may be rewritten:

$$\frac{I_{\lambda, T}}{k(\lambda, T)\,[n_e]} = \sum_i Z_i^2\,[n_i] \qquad (3)$$

where $k(\lambda, T)$ contains the explicit temperature and wavelength dependence of Eq. (2). Since the neutral species concentrations are known as functions of temperature, Eq. (3) was used as a linear parametric relation to make a least-squares fit of the data of Fig. 7 to determine the coefficients Z_i^2. For air, it was assumed that the terms involving NO and O_2 could be neglected due to the lower concentration of these species compared to N_2, N and O over the range of temperature considered.

The results of this curve fit are shown by the lines labeled "Kramer (neutrals)" in Fig. 7. The Z^2's values obtained by this analysis from all the data over the wavelength range of 2.35 - 3.88μ are listed in Table 1.

TABLE 1

Species	Z_i^2
N_2	$2.2 \pm 0.3 \times 10^{-2}$
N	$0.9 \pm 0.4 \times 10^{-2}$
O	$0.2 \pm 0.3 \times 10^{-2}$

Although the value of Z^2 for the O atom is essentially undermined, the magnitude is seen to be considerably smaller than for either N_2 or N. This result changes considerably the interpretation of the free-free continuum from air which has been made in the past.[2] The radiation which was previously associated almost entirely with scattering from O atoms now appears to be due to scattering from N_2 and N with O giving a negligible contribution. It should be noted that the inclusion of any contribution from NO would only make the O contribution smaller.

Using the Z's in Table 1 and Eq. (2), the Kramers' radiation from free-free scattering from neutrals has been calculated for the present experimental conditions. The wavelength dependence is shown as the curves in Figs. 5 and 6 for air and nitrogen, respectively. As can be noted, the Kramers' expression does not reproduce the correct wavelength dependence of the data. Alternatively, the Z's may be considered functions of the wavelength. Obviously, caution should be used in attempts to extrapolate these results using Z's determined at specific wavelengths to other spectral regions.

Acknowledgment

The advice and assistance of many of the members of the staff of AERL is gratefully acknowledged. Drs. J. C. Keck, B. Kivel, J.D. Teare, T. Wentink, Jr. and Mr. P. Hammerling all contributed to the interpretations and calculations. Credit is given to Mr. J. Carlson and Mr. J. McEachern who operated the electric arc-driven shock tube, and to Mr. J. Sullivan and Mr. C. Deradourian who operated the combustion-driven shock tube.

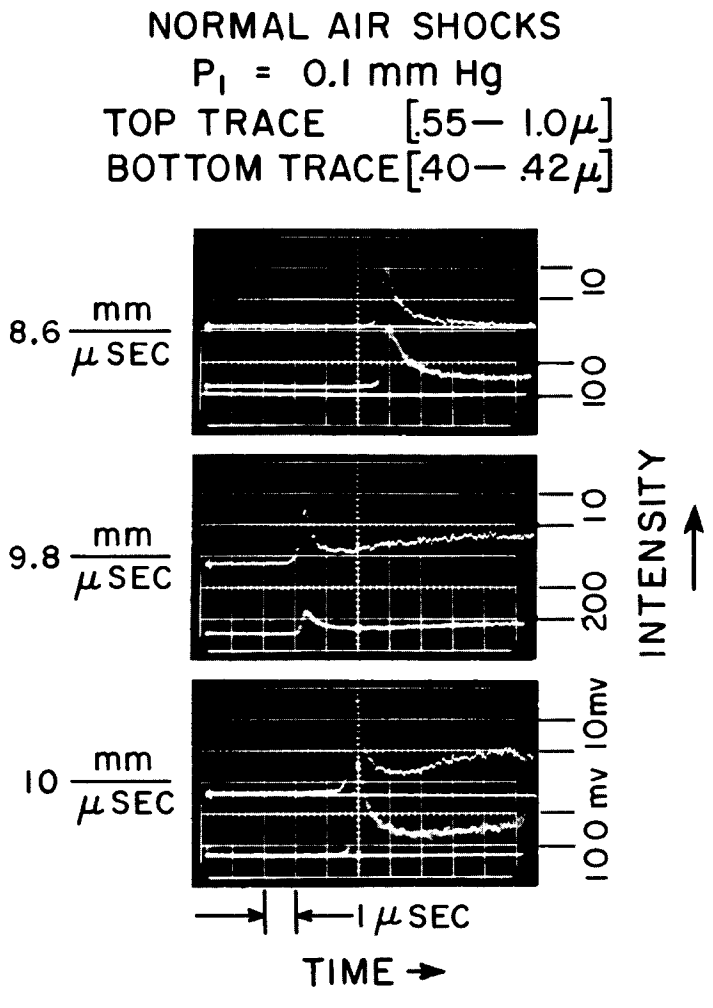

Fig. 1 Oscillogram records of radiation behind normal shocks in air at various shock velocities. The relatively level region behind the radiative overshoot region is taken as the equilibrium region.

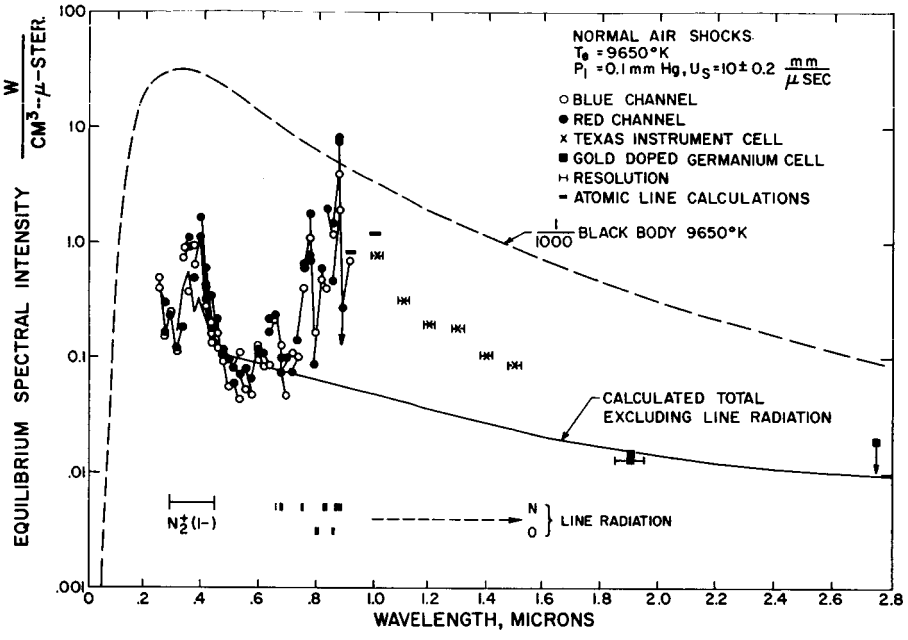

Fig. 2 Equilibrium radiation data obtained by photomultipliers and infrared gauges versus wavelength obtained on incident air shocks U_s = 10 mm/μ sec, P_1 = 0.1 mm Hg. The degree of ionization is about 10%.

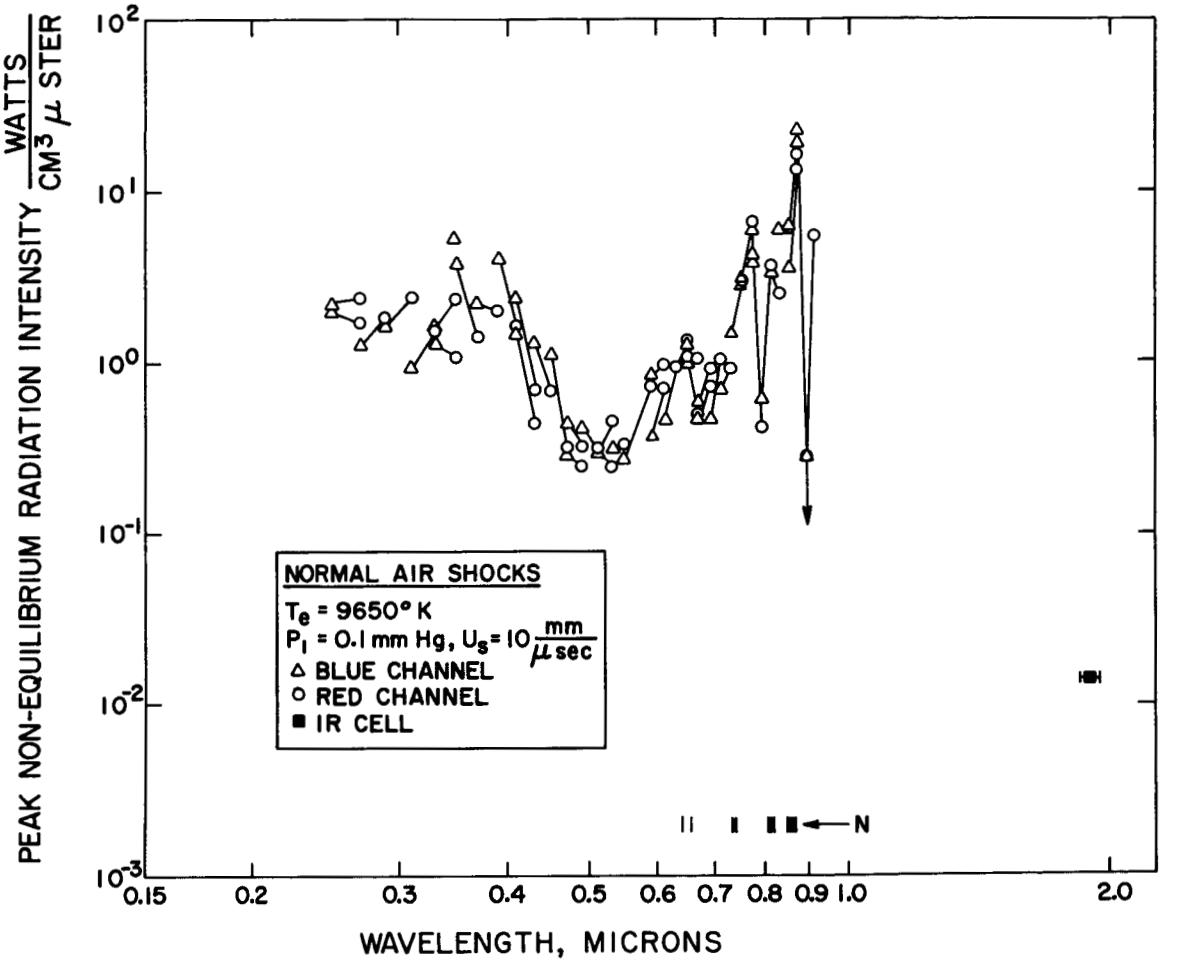

Fig. 3 Absolute intensity measurements versus wavelength at the time of peak radiation in the "overshoot" region behind strong incident air shocks. Atomic line radiation is a prominent feature.

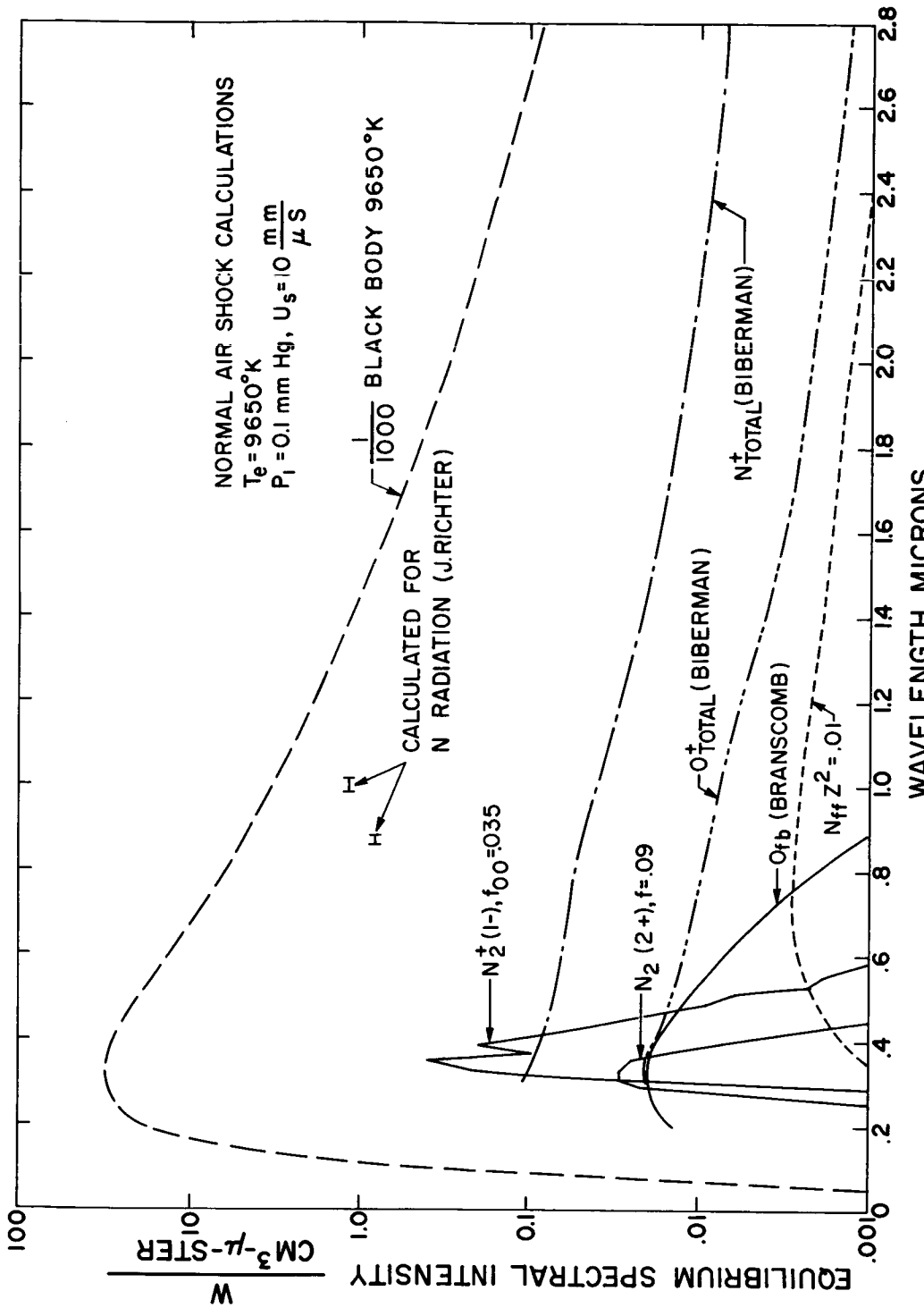

Fig. 4 Calculations of the important radiation which should be the major constituents of the equilibrium radiation behind incident air shocks, U_s = 10 mm/μ sec, P_1 = 0.1 mm Hg.

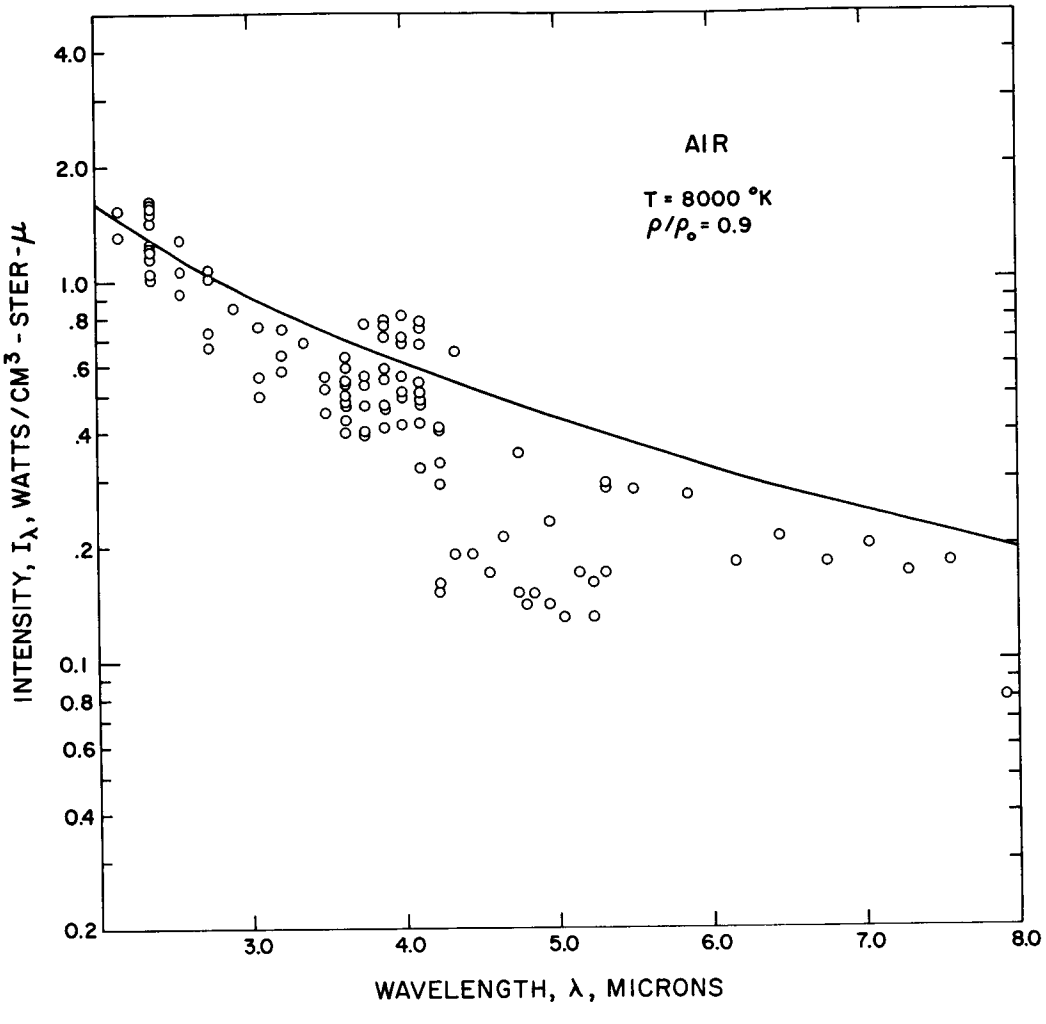

Fig. 5 Absolute intensity of shock-heated air as a function of wavelength. All data have been normalized to a temperature of 8000°K and a density of 0.9 atmospheric. The curve is a calculation of free-free radiation using the classical Kramers' expression with effective Z's determined at $\lambda = 2.35 - 3.88\ \mu$.

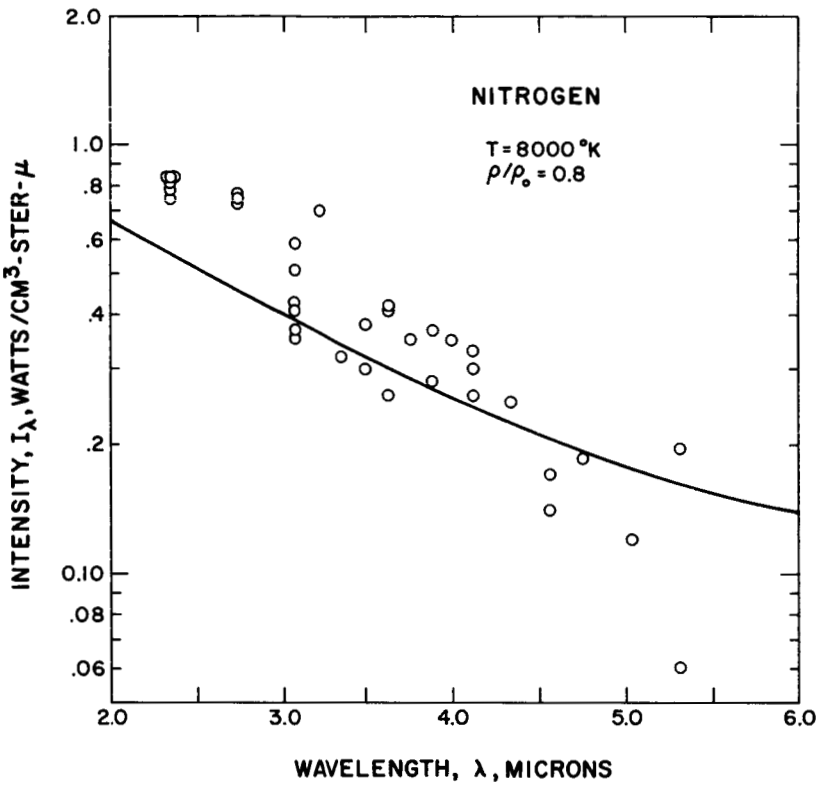

Fig. 6 Absolute intensity of shock-heated nitrogen as a function of wavelength for conditions of 8000°K and 0.8 atmospheric density. The curve is a calculation of the free-free radiation using Kramers' expression with effective Z's determined at $\lambda = 3.07\,\mu$.

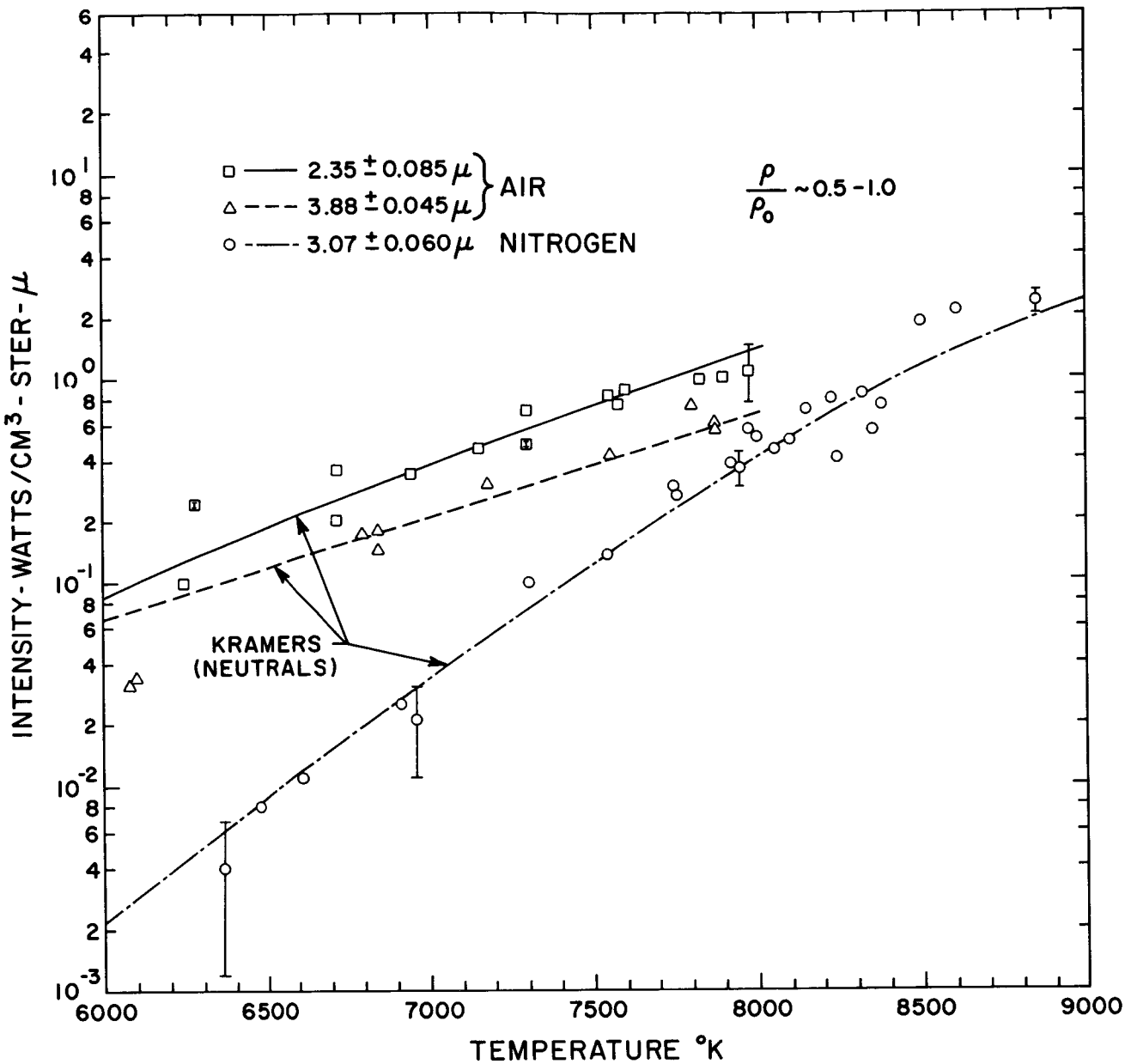

Fig. 7 The temperature dependence of the Bremsstrahlung from air at 2 wavelengths, 2.35 + 0.085 and 3.88 + 0.045μ, and from nitrogen at a wavelength of 3.07 + 0.06 μ. The lines labeled Kramers (neutrals) are least squares curve fits of the data using the Kramers-Unsöld relation, Eq. (3), to determine the effective coulombic charges, Z, for N_2, and N and O.

REFERENCES

1. Camm, J.C., Kivel, B., Taylor, R.L. and Teare, J.D., "Absolute Intensity of Non-Equilibrium Radiation in Air and Stagnation Heating at High Altitudes," J. Quant. Spectr. Rad. Transf. 1:53-75 (Sept. 1961).

2. Wentink, T., Jr., Planet, W., Hammerling P. and Kivel, B., J. Appl. Phys. 29:742 (1958).

3. Camm, J. and Rose, P.H., "Electric Shock Tube for High Velocity Simulation," Avco-Everett Research Laboratory Research Report 136, July 1962.

4. Rose, P.H. and Nelson, W., "On the Effect of Attenuation of Gas Dynamic Measurements Made in Shock Tubes," Avco-Everett Research Laboratory Research Report 24, March 1958; also paper presented at the 2nd Shock Tube Symposium, March 5-6, 1958.

5. Lin, S.C., Neal, R.A. and Fyfe, W.I., "Rate of Ionization Behind Shock Waves in Air. I-Experimental Results.," Avco-Everett Research Laboratory Research Report 105, September 1960.

6. Keck, J.C., Camm, J., Kivel, B. and Wentink, T., Jr. Annals of Phys. 7:1 (1959).

7. Lin, S.C. and Teare, J.D., "Rate of Ionization Behind Shock Waves in Air. II. Theoretical Interpretation," Avco-Everett Research Laboratory Research Report 115, September 1962.

8. Biberman, L.M., Norman, G.E. and Ulyanoo, K.N., "On the Calculation of Photoionization Absorption in Atomic Gases," Opt. i Spektr., 10:565 - 569 (1961).

9. Burgess, A. and Seaton, M.J., "A General Formula for the Calculation of Atomic Photoionization Cross-Sections," Monthly Notices of the Roy. Astron. Soc., 120:121 - 151 (1960).

10. Branscomb, L.M., Burch, B.S., Smith, S.J. and Geltman, S., Photodetachment Cross-Section and the Electron Affinity of Atomic Oxygen," Phys. Rev. 111; 504-513 (1958).

11. Keck. J.C., Allen, R.A. and Taylor, R.L., "Electronic Transition Moments for Air Molecules," Avco-Everett Research Laboratory Research Report 149, March 1963.

12. Richter, J., "On the Oscillator Strengths of Multiplets of Neutral Nitrogen," Zeitschrift für Astrophysik, 51: 177-186 (1961).

13. Wray, K.L., "Chemical Kinetics of High Temperature Air," ARS Report 1975-61; Progress in Astronautics and Rocketry, Vol. 7, ed. by F. R. Riddell, New York: Academic Press (1962). A review.

14. Unsöld, A., Physik der Sternatmospharen, Berlin: Springer (1938).

15. Finkelnburg, W. and Peters, T.H., "Kontinuierliche Spektren," Handbuch der Physik, ed. S. Flugge, Vol. XXVIII, Berlin: Springer, pp. 79-204 (1957).

16. Allen, R.A., Keck, J.C. and Camm, J.C., "Non-Equilibrium Radiation from Shock Heated Nitrogen and a Determination of the Recombination Rate," Avco-Everett Research Laboratory Research Report 110, June 1961; also, Phys. of Fluids 5:284-291, March 1962.